JACS
JOURNAL OF THE AMERICAN CHEMICAL SOCIETY

Article

pubs.acs.org/JACS

Dichotomous Role of Exciting the Donor or the Acceptor on Charge Generation in Organic Solar Cells

Koen H. Hendriks, Alexandra S. G. Wijpkema, Jacobus J. van Franeker, Martijn M. Wienk, and René A. J. Janssen*

Molecular Materials and Nanosystems, Institute for Complex Molecular Systems, Eindhoven University of Technology, P.O. Box 513, 5600 MB Eindhoven, The Netherlands

Dutch Institute for Fundamental Energy Research, De Zaale 20, 5612 AJ Eindhoven, The Netherlands

Supporting Information

ABSTRACT: In organic solar cells, photoexcitation of the donor or acceptor phase can result in different efficiencies for charge generation. We investigate this difference for four different 2-pyridyl diketopyrrolopyrrole (DPP) polymer−fullerene solar cells. By comparing the external quantum efficiency spectra of the polymer solar cells fabricated with either [60]PCBM or [70]PCBM fullerene derivatives as acceptor, the efficiency of charge generation via donor excitation and acceptor excitation can both be quantified. Surprisingly, we find that to make charge transfer efficient, the offset in energy between the HOMO levels of donor and acceptor that govern charge transfer after excitation of the acceptor must be larger by ∼0.3 eV than the offset between the corresponding two LUMO levels when the donor is excited. As a consequence, the driving force required for efficient charge generation is significantly higher for excitation of the acceptor than for excitation of the donor. By comparing charge generation for a total of 16 different DPP polymers, we confirm that the minimal driving force, expressed as the photon energy loss, differs by about 0.3 eV for exciting the donor and exciting the acceptor. Marcus theory may explain the dichotomous role of exciting the donor or the acceptor on charge generation in these solar cells.

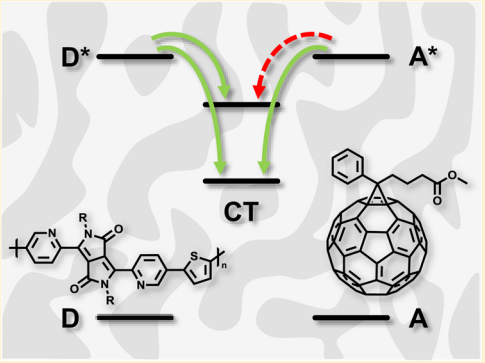

INTRODUCTION

The photocurrent produced by organic solar cells depends on the amount of light absorbed by the active layer, the efficiency dissociating excitons into free charges, and the separation and collection efficiency of these charges. Charge separation may occur after excitation of either the donor or the acceptor.[1] An excited donor can transfer an electron to the acceptor in the ground state and, conversely, an excited acceptor can accept an electron from the donor in the ground state. The latter process is often referred to as hole transfer. The efficiency of charge generation depends on the electron affinity and ionization potential of the donor and acceptor and the excited state energy. In a simplified molecular orbital diagram description, charge transfer from the excited donor relies on the offset between the LUMO energy levels of donor and acceptor (which we will term as Δ_{LUMO}) and, vice versa, the offset between the HOMO levels (i.e., Δ_{HOMO}) governs charge transfer from the excited acceptor. Empirically, it is often assumed that these energy offsets between the frontier orbital levels should be about 0.3 eV to ensure efficient charge separation.[2] In the physically more exact description of a state diagram, the energetics of charge transfer are governed by the energy difference between the interfacial charge transfer (CT) state, E_{CT}, and the optical band gaps or excited state energies of the donor (E_D) and acceptor (E_A).[3] In this case, the sole criterion is that E_{CT} is less than the lowest optical band gap of the donor−acceptor pair ($E_{CT} \leq \min(E_D, E_A)$). If E_D and E_A differ, then charge generation may be preceded by energy transfer, which occurs from the component with the higher optical band gap to the one with the lower gap. In addition, energy barriers can be present that regulate the kinetics of the charge transfer process.[4] Marcus theory provides a description of such barrier in terms of the free energy for charge separation ($E_D - E_{CT}$ or $E_A - E_{CT}$) and the corresponding reorganization energies (λ_D and λ_A).[5] In this description, the barriers for charge transfer originating from the excited donor or the excited acceptor may differ, depending on differences in E_D and E_A or λ_D and λ_A.

In recent years, there is an intense discussion on the role of the photon energy on the quantum efficiency for charge generation.[6,7] This discussion mainly focuses on the question if the interfacial charge transfer state dissociates spontaneously or requires excess energy.[8−11] In many studies, it is often tacitly assumed that the quantum yields for excitation of the donor (electron transfer) or the acceptor (hole transfer) are equal. Although the impact of excitation of the donor or the acceptor on the kinetics for charge generation has been studied in the

Received: June 8, 2016
Published: July 25, 2016

DOI: 10.1021/jacs.6b05868
J. Am. Chem. Soc. 2016, 138, 10026−10031

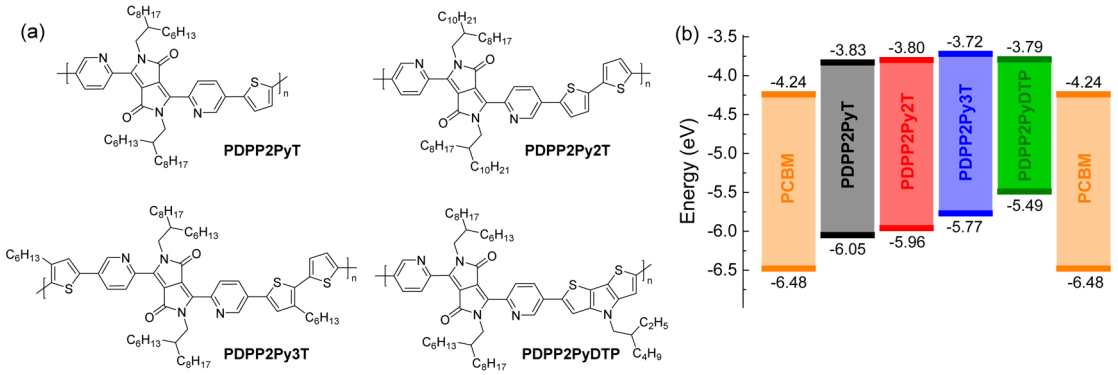

Figure 1. (a) Chemical structure of 2-pyridyl-DPP polymers and (b) Energy level diagram of the polymers compared to [60]PCBM as determined from thin film cyclic voltammetry vs Fc/Fc^{+} (−5.23 eV).

past,[12−14] it is only more recently that attention is growing for the fact that excitation of the donor and acceptor can result in quite different efficiencies for charge generation.[15,16] This difference is sometimes directly observable in the external quantum efficiency (EQE) spectra of polymer (donor) − fullerene (acceptor) solar cells where the absorption bands of the two materials are distinctly different, for instance in diketopyrrolopyrrole (DPP) polymer−fullerene bulk heterojunction solar cells. Several studies reported that PDPP2T-TT/[70]PCBM solar cells have a high EQE of 0.63−0.78 in the wavelength range of fullerene absorption (400−650 nm), while in the region of polymer absorption (650−900 nm) the EQE is more modest at 0.35−0.50.[16−18] This is not due to large differences in absorption of the individual components but rather implies a difference in charge generation efficiency. On the other extreme, recent reports on 2-pyridyl-DPP polymers blended with [70]PCBM show EQE spectra that look remarkably similar to the absorption spectra of the polymer only.[19−21] For these blends, excitation of the fullerene apparently does not contribute significantly to the photocurrent. These remarkable differences prompted us to investigate this phenomenon in more detail. The most pronounced physical difference between these two examples is the position of the HOMO energy level of the polymers and therefore the magnitude of Δ_{HOMO}.

Here we investigate the difference in charge generation efficiency from the excited polymer or the excited fullerene in detail and quantify the generation efficiency of fullerene excitations in DPP polymer/fullerene systems. Specifically, we investigate a series of 2-pyridyl-DPP polymers with varying HOMO energy levels. By comparing the EQE spectra of solar cells made using these polymers as donor with either [60]PCBM or [70]PCBM as acceptor, we identify a clear correlation between the efficiency for charge generation and Δ_{HOMO} when the acceptor is excited. Following the reasoning of different generation efficiencies for excitation of either the donor or the acceptor two, specific energy loss (E_{loss}) terms can be defined, instead of the general definition that $E_{loss} = \min(E_D, E_A) - qV_{oc}$, where q is the elementary charge.[3,22] Hence we introduce $E_{loss,D} = E_D - qV_{oc}$ for excitation of the donor and $E_{loss,A} = E_A - qV_{oc}$ for excitation of the acceptor. We demonstrate that, surprisingly, efficient charge generation in DPP polymer/fullerene systems requires that $E_{loss,A}$ is larger by about 0.3 eV than $E_{loss,D}$. The possible reasons for this remarkable dichotomy are discussed. It introduces a new criterion when designing high efficiency polymers for polymer−fullerene bulk heterojunction solar cells.

RESULTS AND DISCUSSION

The diminished EQE contribution of fullerenes to the photocurrent in the 2-pyridyl-DPP polymer/fullerene systems[19−21] sparked our interest and was chosen as a case study to be investigated in greater detail. To this end a series of polymers with varying HOMO energy levels were synthesized, consisting of disubstituted 2-pyridyl-DPP alternating with progressively stronger electron donors: thiophene < bithiophene < terthiophene < dithienopyrrole. This gave PDPP2PyT, PDPP2Py2T, PDPP2Py3T, and PDPP2PyDTP in high yield and with high molecular weight M_n > 40 kg mol^{-1} (Figure 1a, see Supporting Information (SI) for details on the synthesis and characterization).

The increasing donor strength is well reflected in the HOMO energy levels as determined by cyclic voltammetry measurements (Figure 1b, Figure S2c). The LUMO levels are not much affected by the nature of the donor and lie between −3.72 and −3.83 eV, giving Δ_{LUMO} with PCBM of 0.41−0.52 eV. For the HOMO energy levels, however, we see that the polymers with stronger donors are progressively easier to oxidize, resulting in PDPP2PyT with the deepest HOMO level of −6.05 eV, increasing to −5.96 eV for PDPP2Py2T, − 5.77 eV for PDPP2Py3T, and to −5.49 eV for PDPP2PyDTP. This results in corresponding Δ_{HOMO} with [60]PCBM of 0.43, 0.52, 0.70, and 0.99 eV, respectively.

Solar cells were fabricated using the four polymers by combining them with either [60]PCBM or [70]PCBM as electron acceptor in regular configuration solar cells. LiF/Al was used as top contact. Instead of the conventional PEDOT:PSS bottom contact, a 10 nm MoO_3 on ITO was used as hole extraction layer to prevent S-shaped $J-V$ characteristics that have previously been observed for solar cells with active layers containing aromatic amines such as pyridine and thiazole on PEDOT:PSS.[20,22,23] MoO_3 alleviates this problem. The processing conditions of the polymer/[60]PCBM active layers were carefully optimized in terms of polymer to [60]PCBM ratio, type, and amount of cosolvent, as well as layer thickness to provide the highest power conversion efficiency (PCE). The same processing conditions were then used for the polymer/[70]PCBM blends. Figure 2 and Table 1 show the solar cell characteristics for all material combinations.

The open-circuit voltage (V_{oc}) decreases from ∼1.00 V for PDPP2PyT to ∼0.98 V for PDPP2Py2T, ∼ 0.85 V for PDPP2Py3T, and ∼0.72 V for PDPP2PyDTP and follows the trend in HOMO energy levels of the polymers reasonably well. Although the V_{oc} of the PDPP2PyT cell is high, it is very similar

DOI: 10.1021/jacs.6b05868
J. Am. Chem. Soc. 2016, 138, 10026−10031

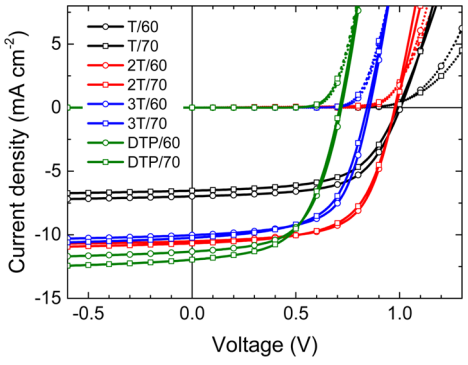

Figure 2. $J-V$ curves of PDPP2PyT, PDPP2Py2T, PDPP2P3T, and PDPP2PyDTP with [60]PCBM (open circles) and [70]PCBM (open squares).

to the V_{oc} of the PDPP2Py2T cell. Judging from the HOMO energy level difference between these polymers an even higher V_{oc} would be expected for PDPP2PyT. The lower steepness of the injection current at the onset in the dark $J-V$ measurement indicates that there might still be a suboptimal interface between PDPP2PyT and the MoO_3 interlayer, suggesting an even higher open-circuit voltage is possible when this interface is further improved. The fill factors for all cells are similar lying between 0.56 and 0.64; the short-circuit current densities vary between 7.00 and 12.6 mA cm^{-2}. As a result, appreciable PCEs are obtained for all material combinations, with PDPP2Py2T/[60]PCBM giving the highest performance of 7.1%. This represents the highest reported efficiency to date for a 2-pyridyl-DPP polymer solar cell. The high performance of PDPP2Py2T is attributed to the high molecular weight of the polymer resulting in a favorable morphology and high J_{sc}, while the $E_{loss,D}$ of 0.76 eV is reasonably low.[3,24,25]

Because of its higher optical absorption coefficient, [70]PCBM based cells generally provide higher performance than [60]PCBM based cells.[26] A closer look at the differences between the [60]PCBM and [70]PCBM cells for each pyridine DPP polymer reveals that, in general, a marginally lower V_{oc} and FF is obtained for the [70]PCBM cells. The more striking observation, however, is that the photocurrent is not significantly increased when replacing [60]PCBM by [70]PCBM. For PDPP2PyT, the photocurrent of the [60]PCBM cell is even higher than that of the [70]PCBM cell. For PDPP2Py2T and PDPP2Py3T a similar photocurrent is obtained, and only for PDPP2PyDTP an increase of ∼1 mA cm^{-2} is measured when using [70]PCBM. Therefore, only the PDPP2PyDTP polymer gives a higher PCE when combined with [70]PCBM than when combined with [60]PCBM.

The EQEs of the solar cells with [60]PCBM and [70]PCBM are virtually identical in the wavelength range above 600 nm where the polymer is the main absorber (Figure 3a). Together with the small differences in V_{oc} and FF between the cells, we therefore conclude that the [60]PCBM and [70]PCBM cells primarily differ by the optical absorption of the fullerene. Since the energy levels of the two fullerene derivatives are identical (Figure S2c),[12] the difference in absorption profile allows to conveniently evaluate the efficiency of hole transfer from fullerene to the polymer. Since the [60]PCBM and [70]PCBM cells have very similar active layer thicknesses, the contribution of the fullerene to the photocurrent can be determined by comparing the EQE spectra of the [60]PCBM and [70]PCBM cells directly. Figure 3a clearly shows that the contribution of the [70]PCBM absorption to the photocurrent between 400 and 550 nm increases in the order PDPP2PyT < PDPP2Py2T < PDPP2Py3T < PDPP2PyDTP, which is in the same order as Δ_{HOMO} (Table S1). This trend is not related to the amount of light absorbed by the various active layers as evidenced from the reflection spectra of the films (Figure S4). The trend is also not related to the morphology, because this does not significantly differ between the [60]PCBM and [70]PCBM cells (Figure S5). Moreover, there is no clear relation between the EQE between 400 and 550 nm and the coarseness of the phase separation between the four blends. Since PDPP2PyT, PDPP2Py2T, and PDPP2Py3T have an optical band gap that is similar to the optical band gap of PCBM (∼1.75 eV), also resonance energy transfer is an unlikely pathway for fullerene exciton separation. Only for PDPP2PyDTP this process might occur since the band gap of this polymer is significantly smaller. We therefore solely relate this observed trend to the difference in energy level between the HOMO level of the fullerene and that of the polymer.

[70]PCBM has an absorption maximum at 480 nm in thin films, whereas [60]PCBM does not significantly absorb 480 nm light. Subtracting the EQE values at 480 nm of the respective [70]PCBM and [60]PCBM cells gives a relative measure of how efficient the fullerene phase is generating charges. Figure 3b shows this ΔEQE_{480} as a function of Δ_{HOMO} and reveals that the charge generation efficiency of fullerene excitations decreases strongly when decreasing Δ_{HOMO}. On the basis of the cyclic voltammetry measurements (Figure 1b), this implies that $\Delta_{HOMO} > 0.4$ eV is required for any charge generation to occur and has to be as high as 0.7 eV for any significant contribution ($\Delta EQE_{480} \approx 0.1$) of the fullerene excitations to the photocurrent. This is in sharp contrast to the charge generation from the polymer which at a Δ_{LUMO} of 0.4−0.5 eV already has high current generation as evidenced from the high

Table 1. Solar Cell Characteristics of 2-Pyridyl DPP Polymer/PCBM Devices

active layer (polymer/PCBM)	d (nm)	V_{oc} (V)	J_{sc}[a] (mA cm^{-2})	FF	EQE_{max}	EQE_{480}	$E_{loss,D}$ (eV)	$E_{loss,A}$ (eV)	PCE (%)
PDPP2PyT/[60]	110	1.000	7.48	0.616	0.481	0.206	0.740	0.750	4.61
PDPP2PyT/[70]	110	0.993	7.00	0.596	0.455	0.222	0.747	0.757	4.14
PDPP2Py2T/[60]	124	0.977	11.34	0.644	0.704	0.365	0.763	0.773	7.13
PDPP2Py2T/[70]	122	0.981	11.38	0.614	0.677	0.421	0.759	0.769	6.85
PDPP2Py3T/[60]	115	0.855	11.10	0.629	0.643	0.355	0.885	0.895	5.97
PDPP2Py3T/[70]	113	0.843	11.24	0.599	0.598	0.461	0.897	0.907	5.68
PDPP2PyDTP/[60]	123	0.719	11.68	0.580	0.563	0.289	0.821	1.031	4.87
PDPP2PyDTP/[70]	128	0.711	12.61	0.560	0.544	0.427	0.829	1.039	5.02

[a]Determined by integrating the EQE spectrum with the AM1.5 G spectrum.

DOI: 10.1021/jacs.6b05868
J. Am. Chem. Soc. 2016, 138, 10026−10031

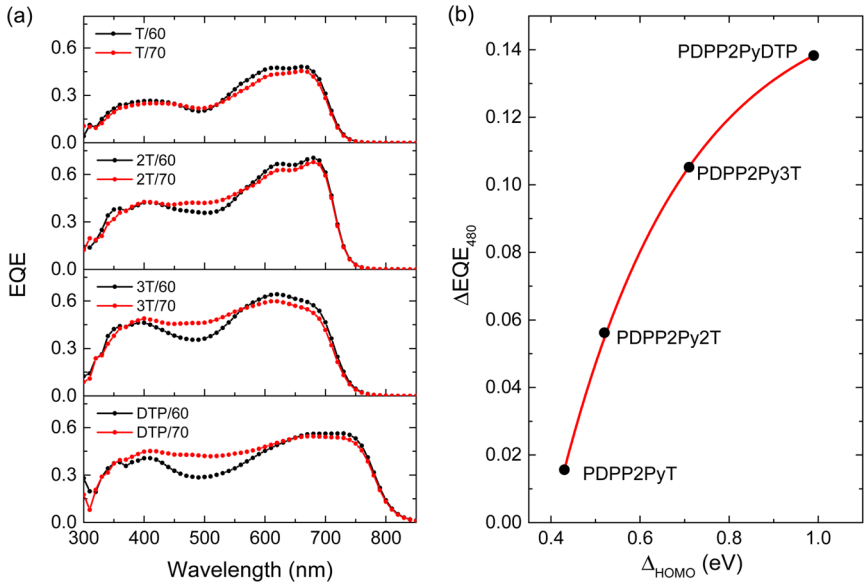

Figure 3. (a) EQE of solar cells of PDPP2PyT, PDPP2Py2T, PDPP2P3T, and PDPP2PyDTP with [60]PCBM and [70]PCBM. (b) ΔEQE_{480} plotted versus Δ_{HOMO} for the 2-pyridyl-DPP polymers and PCBM. The line is a guide to the eye.

EQE_{max} (>0.45) in the polymer absorption region for each of the four polymers.

Apart from using the HOMO energy levels to rationalize the observed trend, the results can be presented in a more general form by using the energy loss term $E_{loss,A}$. $E_{loss,A}$ does not rely on determining the HOMO or LUMO energy levels of the individual components, which are generally dependent on the chosen measuring technique and vacuum level energy. In contrast, $E_{loss,A}$ is determined by the open-circuit voltage of the cell and the optical band gap of the fullerene acceptor. Both parameters can be determined easily and accurately. In Figure 4

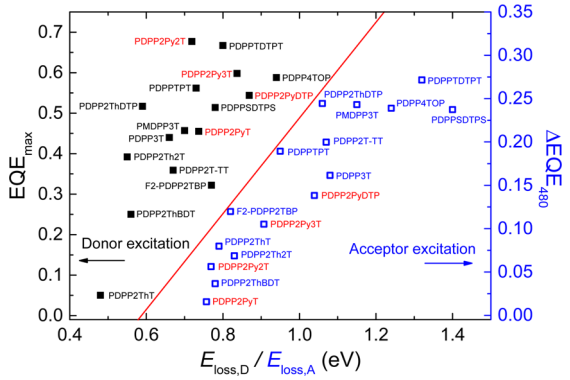

Figure 4. $E_{loss,D}$ versus EQE_{max} (solid squares) and $E_{loss,A}$ versus ΔEQE_{480} (open squares) for the 2-pyridyl DPP polymers (red) and other DPP polymers (black, blue). The red line is a guide to the eye and separates the data for excitation of the polymer donor (left) from those for excitation of the fullerene acceptor (right).

$E_{loss,A}$ is plotted against ΔEQE_{480} for the four 2-pyridyl-DPP polymers presented here and 12 other DPP polymers for which data of comparable [60]PCBM and [70]PCBM cells were available or were measured (Figure S6). In addition, Figure 4 shows the maximum EQE value in the polymer absorption band (EQE_{max}) versus $E_{loss,D}$ for the polymer/[70]PCBM cells. The results clearly show that the trend seen in the 2-pyridyl-DPP polymer series holds for all 16 DPP polymer systems and is present in a large range (0.75−1.4 eV) of energy loss values. Only at high fullerene photon energy losses a significant contribution of fullerene excitations to the photocurrent is observed. There is no apparent correlation between generation of charges via exciting the polymer (EQE_{max}) and exciting the fullerene (ΔEQE_{480}), indicating that the two processes are different. To give an impression of the impact on the solar cell performance, a ΔEQE_{480} of 0.2 amounts to ~2 mA/cm^{-2} difference in current density between [60]PCBM and [70]PCBM cells, which in turn can result in a relative PCE difference of >10%. Figure 4 shows that the minimum $E_{loss,D}$ at which charges are generated is smaller by about 0.3 eV than the minimum $E_{loss,A}$.

We also considered whether the higher $E_{loss,A}$ required for efficient charge generation holds for polymer/fullerene systems in which the polymer is not a DPP material. For this we checked results reported in the literature. We note that the method of determining ΔEQE_{480} requires cells of identical thickness and that there should not be a significant difference in morphology when changing between [60]PCBM and [70]PCBM. These criteria might not always be met for the polymer/fullerene systems considered. Nevertheless, we did not find an example for non-DPP based polymer/fullerene solar cells in which $E_{loss,A}$ is less than ~0.8 eV and where there is still appreciable charge generation via excitation of the fullerene. Representative examples are shown in Figure S7. Although the results in Figure S7 do not show a clear relation between $E_{loss,A}$ and ΔEQE_{480}, the graph confirms that appreciable charge generation via excitation of the fullerene requires $E_{loss,A} \geq 0.85$ eV. This can be compared to the lowest $E_{loss,D}$ reported for a non-DPP polymer of 0.5 eV.[27] Hence, the difference between the minimal $E_{loss,A}$ and $E_{loss,D}$ required for charge generation found for DPP polymer/fullerene cells, might have a more general footing, although this obviously requires more research.

Presently we can only speculate on the origin of the additional (about 0.3 eV) driving force energy required for the separation of fullerene excitons compared to excitons on the polymer chains. According to Marcus theory the rate constant for charge transfer is the product of the electronic coupling and

DOI: 10.1021/jacs.6b05868
J. Am. Chem. Soc. 2016, 138, 10026−10031

an exponential term depending on the activation barrier $\Delta G^{\ddagger}$. Both terms can play a role in explaining the observed differences. The electronic coupling between the initial excited state (D* or A*) and the final charge-transfer (CT) state can be expressed as $\langle \psi_{D^*} | \hat{H} | \psi_{CT} \rangle$ and $\langle \psi_{A^*} | \hat{H} | \psi_{CT} \rangle$ for donor and acceptor excitation, respectively. If the wave function of the exciton in the fullerene acceptor phase is more delocalized than an exciton on the polymer donor, the latter term can be significantly smaller than the first because ψ_{A^*} is smaller than ψ_{D^*} at the polymer/fullerene interface. The concurrent loss in the charge transfer rate can be compensated by reducing the activation barrier for charge transfer $\Delta G^{\ddagger}$ by lowering the energy of the CT state E_{CT}. The second effect that can explain the different efficiency for charge transfer after excitation of the donor or acceptor is a difference in the reorganization energies for the donor (λ_D) and acceptor (λ_A). In Marcus theory the activation barrier $\Delta G^{\ddagger}$ scales with $(E_X - E_{CT} - \lambda_X)^2/4\lambda_X$ (with X = D or A). The term $(E_X - E_{CT})$ scales linearly with $E_{loss,X} = (E_X - qV_{oc})$ because the V_{oc} and E_{CT} are independent of whether the donor or the acceptor is excited. Hence if $E_D = E_A$, or equivalently $E_{loss,D} = E_{loss,A}$, then a different barrier for charge transfer can only result when $\lambda_D \neq \lambda_A$. If a high barrier $\Delta G^{\ddagger}$ exists for charge transfer after excitation of the acceptor, then it can be lowered by lowering the energy of the charge-transfer energy using a better donor, which is equivalent to reducing the open-circuit voltage and increasing E_{loss}. Summarizing, both a difference in electronic coupling and in reorganization energy, can result in different efficiencies for charge transfer after donor or acceptor excitation. Both can be compensated by de lowering the CT energy, resulting in loss of V_{oc}. Additional research will have to point out which exact mechanism causes the dichotomous role of exciting the donor or acceptor. However, it is clear that it is important to not only improve charge generation from the donor, but also from the acceptor phase in order to achieve the highest possible performance from bulk heterojunction solar cells.

CONCLUSION

Four 2-pyridyl-DPP donor polymers with varying HOMO energy levels have been synthesized. The corresponding bulk heterojunction solar cells were fabricated with [60]PCBM and [70]PCBM as acceptor. By comparing the EQE spectra of the [60]PCBM and [70]PCBM solar cells, it is possible to quantify the charge generation efficiency via excitation of the fullerene by comparing the EQE at 480 nm (ΔEQE_{480}). We find that ΔEQE_{480} increases with increasing energy offset between the HOMO levels (Δ_{HOMO}) of the two components in the cells. In fact, charge generation via excitation of the acceptor hardly occurs when $\Delta_{HOMO} < 0.7$ eV. In contrast, excitation of the donor readily produces charges at $\Delta_{LUMO} = 0.4$ eV. As a consequence, the driving force, or minimum photon energy loss E_{loss}, to generate charges efficiently via excitation of the fullerene acceptor is about 0.3 eV higher for exciting the donor. Among 16 DPP polymers with widely different energy levels there was no exception.

These differences in energy loss between the acceptor and donor point toward separate pathways for charge generation from the two components and indicates the presence of two different energy barriers. Following Marcus theory this could be due to a lower electronic coupling at the donor/acceptor interface when exciting the acceptor, or to a difference in reorganization energy of the donor and acceptor in the excited state. Further research will be required to elucidate the mechanism and the wider applicability of the results in more detail. The important conclusion, however, is that both charge generation pathways will have to be optimized in terms of energy loss in order to achieve the highest performing solar cells.

EXPERIMENTAL SECTION

The detailed synthesis and characterization of the monomers and polymers are described in the SI. [60]PCBM (99%) and [70]PCBM (90–95%) were obtained from Solenne BV. Cyclic voltammetry was performed under an inert atmosphere with a scan speed of 0.1 V s^{-1} in an acetonitrile solution of 1 M tetrabutylammonium hexafluorophosphate. An ITO glass slide covered with a thin layer of polymer or PCBM (approximately 20 nm) was used as working electrode, a silver rod as counter electrode, and silver rod coated with silver chloride (Ag/AgCl) as quasi-reference electrode in combination with Fc/Fc^+ as an internal standard. Oxidation and reduction potentials were determined at the onset of the redox waves in the first voltage cycle.

Photovoltaic devices with an active area of 0.09 and 0.16 cm^2 were fabricated by thermally evaporating a 10 nm layer of MoO_3 under high vacuum (~3×10^{-7} mbar) onto precleaned, patterned indium tin oxide (ITO) glass substrates (Naranjo Substrates). The active layer was deposited by spin coating the appropriate polymer/PCBM solutions and transferring the substrates directly to vacuum after deposition. The PDPP2PyT and PDPP2PyDTP coating solutions contained 6 mg mL^{-1} polymer, 12 mg mL^{-1} [60] or [70]PCBM and 5 vol % diiodooctane in chloroform. PDPP2Py2T solutions contained 3 mg mL^{-1} polymer, 6 mg mL^{-1} [60] or [70]PCBM and 3 vol % 1-chloronaphthalene in chloroform. PDPP2Py3T solutions contained 6 mg mL^{-1} polymer, 12 mg mL^{-1} [60] or [70]PCBM and 5 vol % 1-chloronaphthalene in chloroform. The back electrode consisted of LiF (1 nm) and Al (100 nm) which were deposited by evaporation under high vacuum (~3×10^{-7} mbar). The thickness of the active layers was determined on a Veeco Dektak150 profilometer.

J–*V* characteristics were measured with a Keithley 2400 source meter under ~100 mW cm^{-2} white light illumination from a tungsten-halogen lamp filtered by a Schott GG385 UV filter and a Hoya LB120 daylight filter. Short-circuit currents under AM1.5G conditions were determined by convoluting the spectral response with the solar spectrum. Spectral response measurements were conducted under 1 sun operating conditions by using a 530 nm high power LED (Thorlabs) for bias illumination. The device was kept in a nitrogen filled box behind a quartz window and irradiated with modulated monochromatic light, from a 50 W tungsten-halogen lamp (Philips focusline) and monochromator (Oriel, Cornerstone 130) with the use of a mechanical chopper. The response was recorded as a voltage from a preamplifier (SR570) using a lock-in amplifier (SR830). A calibrated silicon cell was used as reference

ASSOCIATED CONTENT

Supporting Information

The Supporting Information is available free of charge on the ACS Publications website at DOI: 10.1021/jacs.6b05868.

Detailed synthesis and characterization of the polymers, reflection spectra of the solar cells, TEM images of the active layers, additional EQE spectra of other DPP polymers with [60]PCBM and [70]PCBM, and literature examples of ΔEQE_{480} of other polymer blends (PDF)

AUTHOR INFORMATION

Corresponding Author

*r.a.j.janssen@tue.nl

Notes

The authors declare no competing financial interest.

DOI: 10.1021/jacs.6b05868
J. Am. Chem. Soc. 2016, 138, 10026–10031

■ ACKNOWLEDGMENTS

The work was supported by the Deutsche Forschungsgemeinschaft under the Priority Programme SPP 1355 "Elementary Processes of Organic Photovoltaics" (JA 1563/1-3). The work of JJvF forms part of the research programme of the Dutch Polymer Institute (DPI), project #734. The research has further received funding from the European Research Council under the European Union's Seventh Framework Programme (FP/2007-2013)/ERC Grant Agreement No. 339031, forms part of the Solliance programme, and has received funding from the Ministry of Education, Culture and Science (Gravity program 024.001.035).

■ REFERENCES

(1) Halls, J. J. M.; Cornil, J.; dos Santos, D. A.; Silbey, R.; Hwang, D. H.; Holmes, A. B.; Brédas, J. L.; Friend, R. H. *Phys. Rev. B: Condens. Matter Mater. Phys.* **1999**, *60*, 5721−5727.
(2) Scharber, M. C.; Mühlbacher, D.; Koppe, M.; Denk, P.; Waldauf, C.; Heeger, A. J.; Brabec, C. J. *Adv. Mater.* **2006**, *18*, 789−794.
(3) Veldman, D.; Meskers, S. C. J.; Janssen, R. A. J. *Adv. Funct. Mater.* **2009**, *19*, 1939−1948.
(4) Clarke, T. M.; Durrant, J. R. *Chem. Rev.* **2010**, *110*, 6736−6767.
(5) Brédas, J. L.; Beljonne, D.; Coropceanu, V.; Cornil, J. *Chem. Rev.* **2004**, *104*, 4971−5004.
(6) For a review: Gao, F.; Inganäs, O. *Phys. Chem. Chem. Phys.* **2014**, *16*, 20291−20304.
(7) For a review: Bässler, H.; Köhler, A. *Phys. Chem. Chem. Phys.* **2015**, *17*, 28451−28462.
(8) Bakulin, A. A.; Rao, A.; Pavelyev, V. G.; van Loosdrecht, P. H. M.; Pshenichnikov, M. S.; Niedzialek, D.; Cornil, J.; Beljonne, D.; Friend, R. H. *Science* **2012**, *335*, 1340−1344.
(9) Lee, J.; Vandewal, K.; Yost, S. R.; Bahlke, M. E.; Goris, L.; Baldo, M. A.; Manca, J. V.; Van Voorhis, T. *J. Am. Chem. Soc.* **2010**, *132*, 11878−11880.
(10) Vandewal, K.; Albrecht, S.; Hoke, E. T.; Graham, K. R.; Widmer, J.; Douglas, J. D.; Schubert, M.; Mateker, W. R.; Bloking, J. T.; Burkhard, G. F.; Sellinger, A.; Fréchet, J. M. J.; Amassian, A.; Riede, M. K.; McGehee, M. D.; Neher, D.; Salleo, A. *Nat. Mater.* **2013**, *13*, 63−68.
(11) Schulze, M.; Hänsel, M.; Tegeder, P. *J. Phys. Chem. C* **2014**, *118*, 28527−28534.
(12) Wienk, M. M.; Kroon, J. M.; Verhees, W. J. H.; Knol, J.; Hummelen, J. C.; van Hal, P. A.; Janssen, R. A. J. *Angew. Chem., Int. Ed.* **2003**, *42*, 3371−3375.
(13) Cook, S.; Katoh, R.; Furube, A. *J. Phys. Chem. C* **2009**, *113*, 2547−2552.
(14) Bakulin, A. A.; Hummelen, J. C.; Pshenichnikov, M. S.; van Loosdrecht, P. H. M. *Adv. Funct. Mater.* **2010**, *20*, 1653−1660.
(15) Ren, G.; Schlenker, C. W.; Ahmed, E.; Subramaniyan, S.; Olthof, S.; Kahn, A.; Ginger, D. S.; Jenekhe, S. A. *Adv. Funct. Mater.* **2013**, *23*, 1238−1249.
(16) Armin, A.; Kassal, I.; Shaw, P. E.; Hambsch, M.; Stolterfoht, M.; Lyons, D. M.; Li, J.; Shi, Z.; Burn, P. L.; Meredith, P. *J. Am. Chem. Soc.* **2014**, *136*, 11465−11472.
(17) Li, W.; Hendriks, K. H.; Furlan, A.; Roelofs, W. S. C.; Wienk, M. M.; Janssen, R. A. J. *J. Am. Chem. Soc.* **2013**, *135*, 18942−18948.
(18) Choi, H.; Ko, S.-J.; Kim, T.; Morin, P.-O.; Walker, B.; Lee, B. H.; Leclerc, M.; Kim, J. Y.; Heeger, A. J. *Adv. Mater.* **2015**, *27*, 3318−3324.
(19) Jung, J. W.; Liu, F.; Russell, T. P.; Jo, W. H. *Chem. Commun.* **2013**, *49*, 8495−8497.
(20) Zhang, X.; Xiao, C.; Zhang, A.; Yang, F.; Dong, H.; Wang, Z.; Zhan, X.; Li, W.; Hu, W. *Polym. Chem.* **2015**, *6*, 4775−4783.
(21) Lee, J. W.; Ahn, H.; Jo, W. H. *Macromolecules* **2015**, *48*, 7836−7842.
(22) Li, W.; Hendriks, K. H.; Furlan, A.; Wienk, M. M.; Janssen, R. A. J. *J. Am. Chem. Soc.* **2015**, *137*, 2231−2234.
(23) Sakthivel, P.; Kranthiraja, K.; Saravanan, C.; Gunasekar, K.; Kim, H. I.; Shin, W. S.; Jeong, J.-E.; Woo, H. Y.; Jin, S.-H. *J. Mater. Chem. A* **2014**, *2*, 6916−6921.
(24) van Franeker, J. J.; Heintges, G. H. L.; Schaefer, C.; Portale, G.; Li, W.; Wienk, M. M.; van der Schoot, P.; Janssen, R. A. J. *J. Am. Chem. Soc.* **2015**, *137*, 11783−11794.
(25) Hendriks, K. H.; Heintges, G. H. L.; Gevaerts, V. S.; Wienk, M. M.; Janssen, R. A. J. *Angew. Chem., Int. Ed.* **2013**, *52*, 8341−8344.
(26) Yamanari, T.; Taima, T.; Sakai, J.; Saito, K. *Jpn. J. Appl. Phys.* **2008**, *47*, 1230−1233.
(27) Kawashima, K.; Tamai, Y.; Ohkita, H.; Osaka, I.; Takimiya, K. *Nat. Commun.* **2015**, *6*, 10085.

DOI: 10.1021/jacs.6b05868
J. Am. Chem. Soc. 2016, 138, 10026−10031